Structural Chemistry (2023) 34:1973–1984
https://doi.org/10.1007/s11224-023-02152-w

RESEARCH

Experimental and computational studies of tautomerism pyridine carbonyl thiosemicarbazide derivatives

Paweł Kozyra[1] · Agnieszka Kaczor[2,3] · Zbigniew Karczmarzyk[4] · Waldemar Wysocki[4] · Monika Pitucha[1]

Received: 3 January 2023 / Accepted: 20 February 2023 / Published online: 7 March 2023

Abstract

Tautomerism is one of the most important phenomena to consider when designing biologically active molecules. In this work, we use NMR spectroscopy, IR, and X-ray analysis as well as quantum-chemical calculations in the gas phase and in a solvent to study tautomerism of 1- (2-, 3- and 4-pyridinecarbonyl)-4-substituted thiosemicarbazide derivatives. The tautomer containing both carbonyl and thione groups turned out to be the most stable. The results of the calculations are consistent with the experimental data obtained from NMR and IR spectroscopy and with the crystalline forms from the X-ray studies. The obtained results broaden the knowledge in the field of structural studies of the thiosemicarbazide scaffold, which will translate into an understanding of the interactions of compounds with a potential molecular target.

Keywords Computational chemistry · X-ray analysis · Tautomerism · Molecular modeling · Thiosemicarbazide

Introduction

The biological activity of the compounds is a function of their physical and chemical parameters which depend on their molecular structure [1]. Thus, it is important to accurately determine the structure of a chemical compound as it will reflect in its molecular properties [2, 3]. An elongation of the alkyl chain may result in a better fit to the active site, thereby increasing the potency of the drug. It could also result in an increase of lipophilicity, which is related to the ease of drug penetration into a molecular target. For example, thioconazole, which is non-polar and poorly soluble in blood, is only used in antifungal skin infections. However, after the introduction of a hydroxyl group and more polar heterocyclic rings, fluconazole was obtained with better solubility and efficiency in systemic fungal infections [4]. On the other hand, the molecular structure, apart from pharmacokinetic properties, also influences pharmacodynamics. For example, the key to local anesthesia is the benzoyl group in the cocaine structure [5]. Thus, it is so important to investigate and precisely determine the structure of the molecule before any biological testing.

One of the important parameters for biological activity is the phenomenon of tautomerism. Antonov calls tautomers chemical chameleons because of their ability to change structure quickly depending on conditions [6]. Prototropic tautomerism is a proton displacement between two polar atoms of a given compound [7]. Related to the low-energy barrier between the tautomers, many factors affect the tautomerization process [8]. It is determined by the ratio of the tautomers, which depends on the molecular structure and the type of chemical compound, solvent, temperature, pressure,

✉ Paweł Kozyra
pawelkozyra@umlub.pl

Agnieszka Kaczor
agnieszka.kaczor@umlub.pl

Zbigniew Karczmarzyk
zbigniew.karczmarzyk@uph.edu.pl

Waldemar Wysocki
waldemar.wysocki@uph.edu.pl

Monika Pitucha
monika.pitucha@umlub.pl

1 Independent Radiopharmacy Unit, Department of Organic Chemistry, Faculty of Pharmacy, Medical University of Lublin, PL-20093 Lublin, Poland

2 Department of Synthesis and Chemical Technology of Pharmaceutical Substances with Computer Modeling Laboratory, Faculty of Pharmacy, Medical University of Lublin, PL-20093 Lublin, Poland

3 School of Pharmacy, University of Eastern Finland, FI-70211 Kuopio, Finland

4 Faculty of Science, University of Natural Sciences and Humanities in Siedlce, PL-08110 Siedlce, Poland

concentration, and pH [7]. The ratio of tautomers determines the most preferred tautomeric form in a particular environment. Tautomers differ in their molecule shapes, proton, and acceptor–donor properties, and therefore, depending on the tautomeric form, they can be involved in different molecular interactions with the molecular targets. In the light of above, determination of the most stable tautomer plays a key role in drug design and discovery.

One of the most common of tautomerism is the keto-enol tautomerism, occurring in the compounds which possess a carbonyl group. In nature, the most common example of keto-enol tautomerism is nitrogen bases, which form hydrogen bonds only by shifting the tautomeric equilibrium into the keto form [9]. Tautomeric equilibrium studies are of great importance because of the key role of tautomerism in the optimization of the biological activity of medicinal compounds [9–16]. The tautomeric form may determine the stability of the ligand, which was, e.g., shown by Senthilkumar and Kolandaivel, who demonstrated greater stability in the polar environment of the bound tautomer with respect to the corresponding unsubstituted barbituric acid tautomer [17]. Temperini et al. proved that tautomeric forms determined the strength of interaction with the active site of an enzyme [18]. They showed that the complex of carbonic anhydrase II with chlorthalidone is bound in the compound lactimic form, instead of the amide form. Many studies focused on keto-enol tautomerism in order to rationalize the biological activity of the tested compounds, assuming that the keto and enol forms may differ in pharmacological activity [4].

Another common type of tautomerism is thione-thiol tautomerism, which occurs in the compounds bearing a thione group (Scheme 1). Jayaram et al. reported that antithyroid drugs are mainly in the form of the thione tautomer [19]. They demonstrated that the tautomeric thione form was related to the presence of the NH group in the structures they studied, which is crucial for the inhibitory effect on lactoperoxidase.

Thiosemicarbazides are a privileged scaffold in medicinal chemistry [20]. Their easy synthesis and broad spectrum of biological activity make them a promising group of therapeutic compounds [21–24]. From the point of view of biological activity, it is very important to study the tautomeric stability of thiosemicarbazides [25–28]. Knowledge of the preferred tautomeric form enables the correct interpretation of the structure–activity relationship (SAR) and molecular docking studies to determine ligand–protein interactions. In order to determine the most stable tautomeric structure, quantum-chemical calculations are often used [29, 30] and the most frequently used method for determining tautomeric stability is DFT [6, 8, 31–34]. Therefore, the use of computational chemistry and structural bioinformatics techniques is of key importance in the contemporary process of drug design and discovery [8, 35]. On the other hand, X-ray crystallography and NMR are also used to determine the structure of chemical compounds [8, 36–40] and to confirm the results of quantum-chemical calculations [16, 35, 41, 42]. Therefore, in our research, we perform a comparison of computational and experimental data.

The aim of our work is to study the phenomenon of tautomerism of pyridine carbonyl thiosemicarbazide derivatives using quantum-chemical calculations in the gas phase and in the solvent environment as IR and NMR spectroscopy and X-ray studies for selected compounds.

Experimental

IR spectra were recorded using a Thermo Nicolet 6700 FTIR spectrometer, with the ATR Diamond Orbit stage. ^{1}H and ^{13}C NMR spectra using DMSO-d_6 as a solvent were recorded using the Bruker AVANCE III 600-MHz, Z-gradient BBO probe spectrometer. The solvent was used as received from a commercial supplier. Tetramethylsilane was applied as an internal standard. B3LYP DFT (a variant of the DFT method using Becke's three-parameter hybrid functional (B3) [43], with a correlation functional such as the one proposed by Lee, Yang, and Parr (LYP) [44], using 6–311 ++ G(3df, 3pd) basis set as included in Gaussian09 [45], was used to optimize the 9 tautomeric structures of compounds **1–9** in the ground state and in DMSO using the Polarizable Continuum Model (PCM) [46, 47]. This approach relies on the overlapping of spheres to form a cavity of the solute. The stabilization energy of the tautomers 01–09 was also calculated for the isolated molecules (gas phase) and molecules in DMSO solutions for all the compounds. When calculating the stabilization energy of the tautomers, the reference was as the least stable tautomer for each compound. The Continuous Set of Gauge Transformations (CSGT) approach [48–50] was used to compute ^{1}H and ^{13}C NMR chemical shifts in DMSO at the same theory level. Next, vibrational frequencies and infrared intensities were also computed. The

Scheme 1 Exemplary tautomeric forms of thiosemicarbazides

IR spectra were rescaled by 0.9608 in accordance with the recommendations for this level of theory [51]. B3LYP DFT method and the 6–311 ++ G(3df, 3pd) basis set of Gaussian09 [17] software were used to calculate the energy of HOMO and LUMO orbitals. GaussView v. 6.0 was applied to visualize HOMO and LUMO orbital shapes. Electrostatic potential distribution was computed and visualized with ArgusLab v. 4.0.1 [52]. Non-covalent interaction maps were calculated with NCIPlot v. 3.0 [53] and visualized with VMD v. 1.9.4 [54], as reported earlier [55].

X-ray data of **9** were collected on the KUMA Diffraction KM-4 CCD diffractometer (MoKα ($\lambda = 0.71073$ Å) radiation, ω scans, $T = 296(2)$ K; crystal sizes $0.50 \times 0.30 \times 0.05$ mm, absorption correction: multi-scan CrysAlisPro [56], T_{min}/T_{max} of 0.7711/1.0000). The structure was solved by direct methods using SHELXS97 [56] and refined by full-matrix least squares with SHELXL-2014/7 [57]. The N-bound H atoms were located by difference Fourier synthesis and refined freely. The remaining H atoms were positioned geometrically and treated as riding on their parent C atoms with C-H distances of 0.93 Å (aromatic). All H atoms were refined with isotropic displacement parameters taken as 1.5 times those of the respective parent atoms. Electron density associated with an additional disordered solvent molecule was removed with the SQUEEZE procedure in PLATON [58] (the solvent-accessible volume of 316 Å3 with 76 electrons in the cavities). All calculations were performed using the WINGX version 1.64.05 package [59]. CCDC-2189746 for **9** contains the supplementary crystallographic data for this paper. These data can be obtained free of charge at www.ccdc.cam.ac.uk/conts/retrieving.html (or from the Cambridge Crystallographic Data Centre (CCDC), 12 Union Road, Cambridge CB2 1EZ, UK; fax: + 44(0) 1223 336 033; email: deposit@ccdc.cam.ac.uk).

Crystal data of C1: C13H10N4OS, $M = 341.21$, monoclinic, space group $P21/c$, $a = 12.7027(9)$, $b = 9.9754(6)$, $c = 13.5119(7)$ Å, $\beta = 90.851(6)$, $V = 1711.96(18)$ Å3, $Z = 4$, $d_{calc} = 1.324$ Mg m^{-3}, $F(000) = 696$, μ(Mo Kα) = 0.503 mm^{-1}, $T = 296$ K, 7580 measured reflections (θ range 2.54–29.07o), 3861 unique reflections, final $R = 0.048$, $wR = 0.121$, $S = 1.027$ for 2773 reflections with $I > 2\sigma(I)$ (Supplement 1).

Results and discussion

Thiosemicarbazides are a very important group of compounds used in organic synthesis to obtain biologically active systems, e.g., triazoles, thiadiazoles, and oxadiazoles [60, 61]. For several years, researchers have focused on thiosemicarbazide derivatives as privileged structures for biological activity. Their antiviral and anthelmintic properties are widely described in the literature [62, 63]. Many compounds from this group exhibit antimicrobial activity against *Klebsiella pneumoniae*, *Staphylococcus aureus*, and *Escherichia coli* comparable to standard antibacterial drugs [64]. Thiosemicarbazide derivatives containing a thiazole ring were screened for inhibitory activity against *Mycobacterium tuberculosis* H37Ra and *Mycobacterium bovis* strains [65].

Our group obtained a series of 1- (2-, 3-, 4-pyridinecarbonyl)-4-substituted thiosemicarbazide derivatives and evaluated their antimicrobial and antitumor activity (Scheme 2) [21, 22].

The title compounds were synthesized in the reaction of 2- or 3- or 4-pyridinecarboxylic acid hydrazide reaction with 4-methylphenyl or 4-nitrophenyl or 2,4-dichlorophenyl isothiocyanate according to the previously described procedure [21, 22]. Biological studies have shown that some of these compounds (**1**, **2**, **4–6**) display antibacterial activity against *Staphylococcus epidermidis*, *Streptococcus mutans*, and *Streptococcus sanguinis* with MIC values in the range of 7.81–62.5 mg/mL and show a therapeutic index higher than that of ethacridine lactate. Furthermore, compound (**3**) potently inhibits the proliferation of HepG2 (human hepatocellular carcinoma) and MCF-7 (human breast adenocarcinoma) cells with an $IC_{50} = 2.09 \pm 0.11$ µM and 8.63 ± 1.75 µM, respectively, in a concentration-dependent manner [21] and (**2**) inhibits A549 (lung adenocarcinoma cell line) with an $IC_{50} = 4.96 \pm 1.96$ µg/mL [22].

Due to the key importance of the influence of physicochemical parameters on biological activity, we decided to investigate the phenomenon of tautomerism for the obtained thiosemicarbazide derivatives. The phenomenon of tautomerism, especially of the proton transfer, plays an important role in modern organic chemistry, biochemistry, drug chemistry, pharmacology, and molecular biology.

Related to the possibility of migration of labile protons from NH groups to carbonyl (C = O) or thione (C = S) groups, the thiosemicarbazide derivatives studied by us may exist in nine tautomeric forms (Fig. 1). We showed in our earlier work that in the solid state, thiosemicarbazides exist in the keto-thione form [22]. Here, we present experimental and computational studies of the tautomerism phenomenon for new biologically active compounds **1–9**.

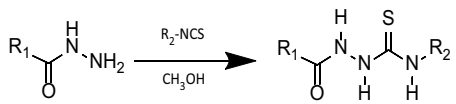

R_1	R_2
pyridin-2-yl	4-$CH_3SC_6H_4$ (**1**), 4-$NO_2C_6H_4$ (**2**), 2,4-$Cl_2C_6H_3$ (**3**)
pyridin-3-yl	4-$CH_3SC_6H_4$ (**4**), 4-$NO_2C_6H_4$ (**5**), 2,4-$Cl_2C_6H_3$ (**6**)
pyridin-4-yl	4-$CH_3SC_6H_4$ (**7**), 4-$NO_2C_6H_4$ (**8**), 2,4-$Cl_2C_6H_3$ (**9**)

Scheme 2 Synthesis of 1-pyridinecarbonyl-4-substituted thiosemicarbazide derivatives (**1–9**)

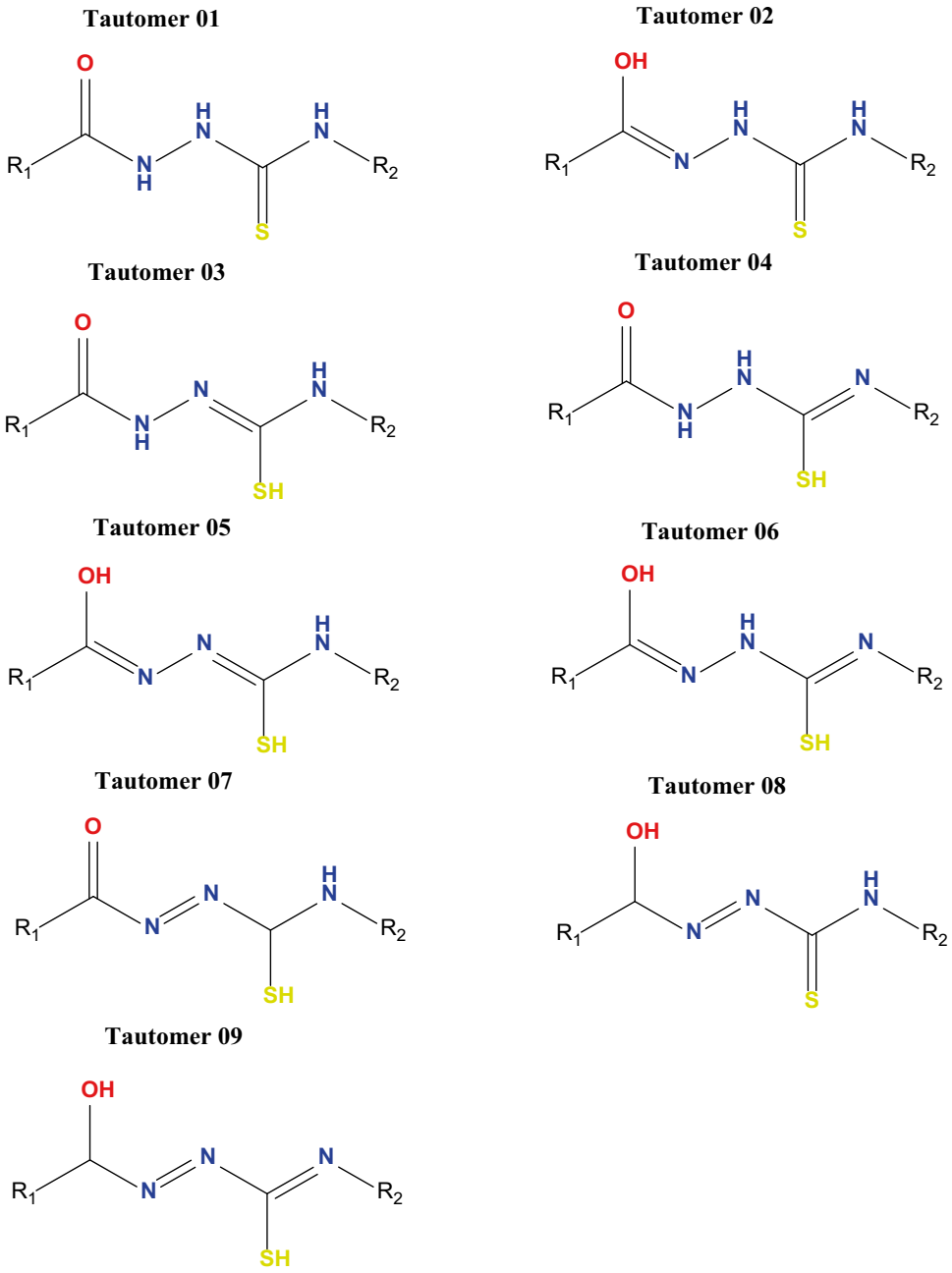

Fig. 1 Possible tautomeric forms of the 1,4-disubstituted thiosemicarbazide derivatives

B3LYP DFT approach and 6–311 ++ G(3df, 3pd) basis set as included in Gaussian09 were used to optimize energy and geometry of compounds **1–9** in the ground state (*in vacuum*) and in DMSO. The stabilization energy values were calculated as the difference between the value of the most stable tautomer and the corresponding one. The population analysis of tautomeric forms was estimated using a non-degenerate Boltzmann distribution. The results of the calculations are presented in Table 1.

The obtained values of energy stabilization indicated that tautomer 01 is the most stable in both the gas phase and DMSO for all the studied compounds, which shows that the presence of ketone and thione groups in the carbonyl thiosemicarbazide system stabilized molecules **1–9** in both considered environments. In the case of compounds **4–6** and **5–9** with pyridyn-3-yl and pyridin-4-yl substituents, respectively, two tautomeric forms 01 and 02 can coexist both in the gas phase and in the solution, wherein the population of them is according to the relation 01 >> 02, with the highest participation of tautomeric form 02 observed for **5** of 1.30% and **8** of 1.28% in the gas phase. In other analyzed cases, the population of the tautomeric forms 02–09 in considered environments is below the threshold of the detectability of conventional analytical methods with the highest stabilization energy for the

Table 1 Stabilization energy E [kcal/mol] and population p_i [%] of tautomers (T) 01–09 of compounds **1–9** in vacuum and DMSO

Comp.		**1**		**2**		**3**		**4**		**5**		**6**		**7**		**8**		**9**	
T		*E*	p_i	*E*	p_i	*E*	p_i	*E*	p_i	*E*	p_i	*E*	p_i	*E*	p_i	*E*	p_i	*E*	p_i
01	Vac	0.00	100.00	0.00	100.00	0.00	100.00	0.00	99.93	0.00	98.70	0.00	99.60	0.00	99.92	0.00	98.72	0.00	99.66
	DMSO	0.00	100.00	0.00	100.00	0.00	100.00	0.00	99.81	0.00	99.68	0.00	99.78	0.00	99.67	0.00	99.39	0.00	99.85
02	Vac	16.11	0.00	14.92	0.00	18.25	0.00	4.23	0.07	2.52	1.30	3.22	0.40	4.17	0.08	2.53	1.28	3.30	0.34
	DMSO	13.23	0.00	11.53	0.00	12.66	0.00	3.66	0.19	3.34	0.32	3.56	0.22	3.33	0.33	2.97	0.61	3.23	0.15
03	Vac	14.04	0.00	12.98	0.00	13.17	0.00	14.19	0.00	12.76	0.00	13.98	0.00	13.83	0.00	12.50	0.00	14.19	0.00
	DMSO	11.83	0.00	10.73	0.00	14.92	0.00	12.64	0.00	10.71	0.00	13.61	0.00	11.69	0.00	10.59	0.00	13.83	0.00
04	Vac	11.84	0.00	10.04	0.00	11.76	0.00	12.48	0.00	10.33	0.00	19.94	0.00	12.61	0.00	10.37	0.00	13.00	0.00
	DMSO	12.99	0.00	11.74	0.00	11.56	0.00	12.92	0.00	11.50	0.00	11.87	0.00	13.14	0.00	11.85	0.00	12.06	0.00
05	Vac	20.73	0.00	19.13	0.00	19.98	0.00	21.24	0.00	20.03	0.00	20.42	0.00	21.64	0.00	19.78	0.00	20.75	0.00
	DMSO	25.16	0.00	22.58	0.00	23.40	0.00	25.20	0.00	22.67	0.00	23.43	0.00	25.41	0.00	22.85	0.00	23.67	0.00
06	Vac	25.23	0.00	21.79	0.00	24.44	0.00	26.86	0.00	23.92	0.00	26.15	0.00	26.90	0.00	23.93	0.00	26.16	0.00
	DMSO	28.84	0.00	23.78	0.00	24.48	0.00	29.19	0.00	25.79	0.00	26.36	0.00	29.28	0.00	25.79	0.00	26.46	0.00
07	Vac	35.48	0.00	34.71	0.00	36.39	0.00	36.53	0.00	34.17	0.00	36.16	0.00	36.69	0.00	34.45	0.00	36.17	0.00
	DMSO	37.48	0.00	36.18	0.00	37.95	0.00	39.16	0.00	36.22	0.00	37.02	0.00	39.35	0.00	35.76	0.00	37.34	0.00
08	Vac	29.58	0.00	30.33	0.00	34.23	0.00	34.96	0.00	36.04	0.00	36.09	0.00	34.59	0.00	35.63	0.00	35.79	0.00
	DMSO	30.36	0.00	33.88	0.00	36.21	0.00	36.27	0.00	37.91	0.00	37.29	0.00	35.83	0.00	37.34	0.00	36.84	0.00
09	Vac	45.00	0.00	42.80	0.00	46.66	0.00	53.29	0.00	52.69	0.00	54.80	0.00	52.78	0.00	52.97	0.00	53.83	0.00
	DMSO	51.38	0.00	48.75	0.00	50.21	0.00	56.14	0.00	55.19	0.00	55.13	0.00	55.46	0.00	57.74	0.00	54.67	0.00

Table 2 Energies of HOMO and LUMO orbitals for the most stable tautomer of compounds **1–9**

Compound	E_{HOMO} (eV)	E_{LUMO} (eV)	LUMO–HOMO gap (eV)
1	− 5.76	− 1.87	3.89
2	− 6.81	− 2.83	3.98
3	− 6.47	− 2.05	4.42
4	− 5.82	− 2.00	3.82
5	− 6.91	− 2.89	4.02
6	− 6.12	− 1.72	4.40
7	− 5.85	− 2.17	3.68
8	− 6.96	− 2.93	4.03
9	− 6.15	− 1.75	4.40

tautomeric form 09, ranging from 42.80 kcal/mol for **2** to 54.80 kcal/mol for **6** in the gas phase and from 48.75 kcal/mol for **2** to 57.74 kcal/mol for **8** in DMSO.

Molecular orbitals and their properties, i.e., energy, are useful for explaining the electronic properties of the compounds. Frontier electron density is often applied for predicting the most reactive position in π-electron systems and to explain a number of reactions in conjugated systems [66].

HOMO (Highest Occupied Molecular Orbital) and LUMO (Lowest Unoccupied Molecular Orbital) energy is often used to determine the chemical reactivity of molecules. During molecular interactions, the LUMO accepts electrons while the HOMO represents electron donors [67]. Energies of HOMO and LUMO as well as LUMO–HOMO gap for the most stable tautomer 01 of compounds **1–9** are presented in Table 2. HOMO and LUMO orbitals for tautomer 01 of the most active compounds **2** and **3** are shown in Fig. 2. It can be seen that for **2**, both HOMO and LUMO orbitals are present on the thiosemicarbazide and phenyl part of the molecule, making it most reactive, in contrast to the pyridyl moiety which is not reactive. The reason for this is the large accumulation of electronegative atoms on one side of the molecule. However, for **3**, the LUMO orbital is stretched into the entire molecule and the distribution of the HOMO orbital is the same as previously described for **2**.

Investigation of protein and ligand electrostatic potential aimed at optimizing electrostatic complementarity is of great importance in drug design [68]. The distribution of electrostatic potential maps for the most stable tautomer 01 of compounds **2** and **3** is presented in Fig. 3. It can be seen that pyridyl nitrogen, the nearby carbonyl oxygen, and nitro group oxygen atoms are the most electronegative part of compound **2**, similarly as for compound **3**, which, however, does not possess a nitro group.

Non-covalent interactions are crucial for the explanation of a number of chemical, biological, and technological problems [53]. A thorough description of these interactions, in particular their positions in real space, is the starting point for decoupling the complex balance of forces that define the interactions [53]. Non-covalent interaction maps for the most stable tautomer 01 of compounds **2** and **3** are presented in Fig. 4. A number of week attracting interactions (green) have been identified for the compounds studied. Furthermore, we studied experimental and computed NMR spectra of the most stable tautomer 01 of compounds **1–9**. ^{1}H NMR spectra for all the derivatives show peaks of N^{7}-H, N^{9}-H, and N^{10}-H at 9.58–10.18 ppm, 9.73–0.27 ppm, and 10.74–11.00 ppm, respectively, which is supported by the literature [55, 69, 70]. The signals in the range of 7.22–9.12 ppm confirmed the presence of two phenyl rings. These signals differed depending on the position of the heteroatom on the phenyl ring and on the type of the second substituent [55, 71].

^{13}C NMR spectra confirmed the presence of carbonyl group (C = O) signal in the range of 163–165 ppm and thione group (C = S) signal in the range of 181–189 ppm. This correlates with the chemical shifts obtained for these atoms by several authors [21, 22, 53, 72–74]. Related to the presence of many highly electronegative atoms, the chemical shifts differ slightly. The most stable tautomer has a carbonyl and a thione group, which is confirmed by these studies. Experimental and

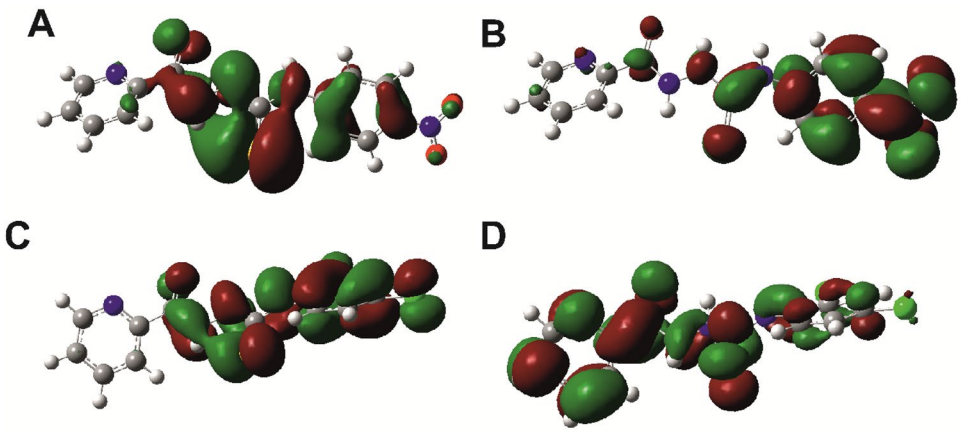

Fig. 2 HOMO (**A**, **C**) and LUMO (**B**, **D**) orbitals for the most stable tautomer of compounds **2** (**A**, **B**) and **3** (**C**, **D**)

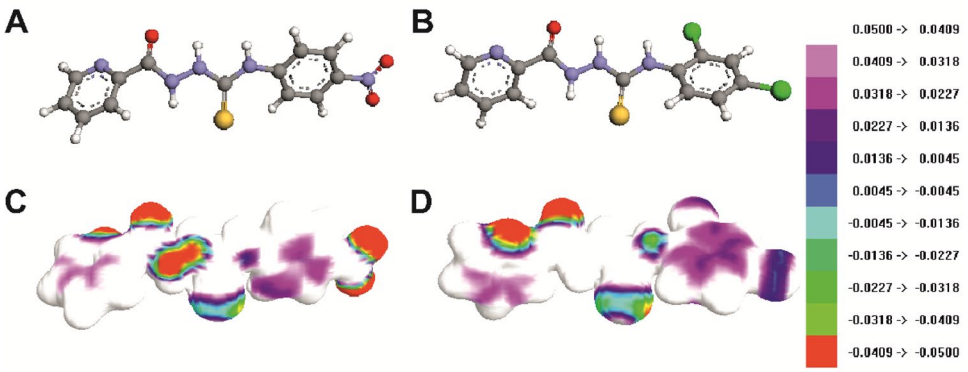

Fig. 3 Molecular structures of the most stable tautomer of compounds **2** (**A**) and **3** (**B**). Electrostatic potential surface for the most stable tautomer of compounds **2** (**C**) and **3** (**D**)

computed ^{1}H and ^{13}C NMR spectra are presented in Table 3 and they correspond well with each other.

We also conducted a detailed analysis of experimental and computed IR spectra of the most stable tautomer 01 for compounds **1–9** (Table 4), as they can provide valuable structural information about the compounds. The presence of a band in the absorption range 3328–2937 cm^{-1} indicates the presence of NH groups. Analysis of the IR spectra confirms the presence of strong absorption band characteristic of the group C = O in the range of 1701–1653 cm^{-1}. Another structural feature of the tested derivatives of thiosemicarbazide is a thione group, which occurs in the spectra in the range of 1307–1296 cm^{-1} [69, 74]. Moreover, the IR spectra of compounds **1–9** did not reveal a C-SH stretching band in the ~ 2600 cm^{-1} range [69], which confirms our assumptions regarding the most likely tautomeric state. The experimental and computed scaled IR frequencies are in good accordance and confirm the energetical preference of tautomer 01 in case of all compounds studied.

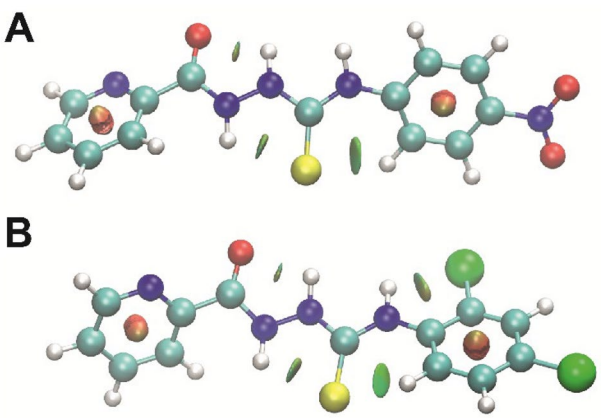

Fig. 4 Non-covalent interaction maps for the most stable tautomer of compounds **2** (**A**) and **3** (**B**). Green spots depict attractive interactions while red spots depict repulsive interactions

In order to confirm the synthesis pathway, the assumed molecular structures, and identification of the tautomeric form in the crystalline state for the compounds obtained, X-ray studies were performed and structures were described for compounds **3**, **4**, and **6** [73]. Here, we presented the crystal and molecular structure of the next, compound **9**, in the investigated series of carbonyl thiosemicarbazides. The molecular structure of **9** in the conformation observed in the crystal is shown in Fig. 5.

The molecule occurs in N1-amino/S3-thione/N4-amino/N5-amino/O7-keto, 01 (Fig. 1), tautomeric form, which is confirmed by the C3–S3 and C5–O5 bond lengths of 1.683(2) and 1.218(3) Å, respectively, typical for the thione and carbonyl groups [75], and the positions of the amino H-atoms at the difference electron-density map in the immediate vicinity of the N1, N4, and N5 atoms. The torsion angles C21–N1–C2–N4, N1–C2–N4–N5, C2–N4–N5–C6, and N4–N5–C6–C31 of − 178.6(2), 5.4(3), 92.7(3), and 176.70(19)o, respectively, show that the carbonyl thiosemicarbazide chain adopts a trans–cis-gauche-trans conformation. The 2,4-dichlorophenyl and pyridyl substituents with respect to the carbonyl thiosemicarbazide system have the gauche and cis conformations, respectively, as shown by the torsion angles C22–C21–N1–C2 of 110.6(3)o and N5–C6–C31–C32 of − 13.8(3)o. The thione C2–S3 group adopts a trans conformation with respect to N4–N5 with the torsion angle N5–N4–C2–S3 of − 176.11(17)o, while the carbonyl C6–O7 group has the cis position with respect to this bond and is practically coplanar with the pyridine ring, as evidenced by the torsion angles N4–N5–C6–O7 and C32–C31–C6–O7 of − 4.9(3) and 167.8(2)o, respectively. In the crystal structures of **9**, the molecular packing is influenced by the net of strong intermolecular hydrogen bonds N1–H1…N34^{i} [N1–H1 = 0.79(3), H1…N34 = 2.22(3), N1…N34 = 2.993(3) Å, N1–H1…N34 = 167(3)o, (i) = 1-x, 1-y, -z], N4–H4…S3^{ii} [N4–H4 = 0.82(3), H4…S3 = 2.52 (3), N4…S3 = 3.312(2) Å, N4–H4…S3 = 166(3)o, (ii) = 1-x, 1-y, 1-z] and N5–H5…O7^{iii} [N5–H5 = 0.76(3), H5…

Table 3 Experimental and computed ^{1}H and ^{13}C NMR chemical shifts for the most stable tautomer 01 of compounds **1–9**

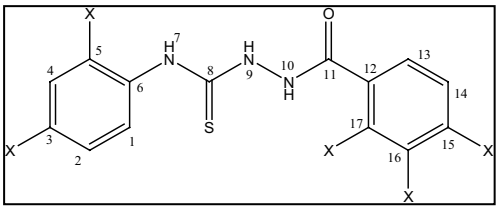

Atom	Compounds and NMR chemical shifts (ppm)																	
	1		**2**		**3**		**4**		**5**		**6**		**7**		**8**		**9**	
	Exp	Calc	Exp	Calc	Exp	Calc	Exp	Calc	Exp	Calc	Exp	Calc	Exp	Calc	Exp	Calc	Exp	Calc
C1	127	133	124	126	128	136	129	133	124	127	128	134	122	135	121	127	128	133
C5	127	133	124	126	127	136	129	133	124	127	133	139	132	135	121	127	133	138
C2	122	130	123	133	128	135	124	130	125	133	129	134	122	135	125	133	129	134
C4	122	130	123	133	129	135	124	130	125	133	129	137	122	135	125	133	132	137
C3	134	149	149	150	127	143	137	149	146	150	133	143	140	143	143	150	133	143
C6	138	141	138	155	123	142	136	141	144	155	136	142	137	142	151	155	140	142
C8	181	181	181	178	182	179	182	181	181	178	183	179	183	179	189	178	182	179
C11	163	168	164	169	164	169	165	167	165	168	165	167	165	167	164	168	165	167
C12	139	159	149	159	149	159	129	134	128	134	132	134	137	146	141	146	137	146
C13	126	129	124	129	123	129	136	141	136	141	137	141	122	127	122	127	122	127
C17	-	-	-	-	-	-	149	159	149	159	149	159	122	127	122	127	122	127
C18	16	19	-	-	-	-	16	19	-	-	-	-	16	19	-	-	-	-
C14	136	145	138	159	149	159	124	130	124	130	124	130	151	160	151	160	151	160
C16	148	159	149	145	149	145	-	-	-	-	-	-	151	160	151	160	151	160
C15	127	133	128	134	127	134	153	162	153	163	153	162	-	-	-	-	-	-
H1	7.26	7.66	7.92	8.13	8.08	8.37	7.38	7.64	7.90	8.11	7.41	8.40	7.38	8.43	7.88	8.11	7.71	8.43
H5	7.26	7.66	7.92	8.13	-	-	7.38	7.64	7.90	8.11	-	-	7.38	8.43	7.88	8.11	-	-
H2	7.40	7.44	8.21	8.79	7.42	7.56	7.24	7.45	8.23	8.11	7.41	7.59	7.24	7.65	8.23	8.79	7.44	7.57
H4	7.40	7.44	8.21	8.79	7.42	7.73	7.24	7.45	8.23	8.79	7.68	7.73	7.24	7.65	8.23	8.79	7.36	7.73
H3	-	-	-	-	-	-	-	-	-	-	-	-	-	-	-	-	-	-
H7	9.73	7.38	10.09	7.79	9.58	7.59	9.81	7.35	10.16	7.77	9.75	7.51	9.84	7.62	10.18	7.79	9.76	7.62
H9	9.73	9.50	10.20	9.85	9.96	9.75	9.81	9.54	10.24	9.88	10.02	9.77	9.84	9.75	10.27	9.83	10.05	9.75
H10	10.74	10.87	10.90	10.83	10.84	10.79	10.77	10.94	10.89	10.91	10.86	11.00	10.85	11.12	11.00	11.08	10.95	11.12
H13	8.07	8.09	8.06	8.10	7.66	8.07	8.28	8.33	8.29	8.37	8.28	8.36	7.85	8.04	7.88	8.03	7.86	8.04
H17	-	-	-	-	-	-	9.11	9.51	9.11	9.52	9.11	9.53	7.85	8.04	7.88	8.03	7.86	8.04
H14	8.02	8.25	8.06	8.27	7.66	8.25	7.56	7.77	7.58	7.79	7.56	7.78	8.78	9.16	8.80	9.17	8.78	9.16
H16	8.60	9.12	8.71	9.14	8.69	9.13	-	-	-	-	-	-	8.78	9.16	8.80	9.17	8.78	9.16
H15	8.02	7.84	7.67	7.87	8.03	7.86	8.76	9.12	8.78	9.15	8.76	9.13	-	-	-	-	-	-
H18	2.46	2.54	-	-	-	-	2.47	2.55	-	-	-		2.47	2.55				

O7 = 2.21(3), N5…O7 = 2.893(3) Å, N5–H5…O7 = 151(3) o, (iii) = 1-x, ½ + y, ½-z], which stabilized the tautomeric form observed in crystal. Moreover, the π…π interaction between pyridine rings within the molecular dimer formed by inversion-related molecules is observed; the centroid-to-centroid separation and the angle between the overlapping planes of these rings are 3.4947(14) Å and 0.03(12) o, respectively. It is worth noting that the intermolecular interactions observed in the crystal are in good agreement with the predicted non-covalent interactions shown in Fig. 4. In our previous research on thiosemicarbazide derivatives, we presented the crystal and molecular structures of several compounds containing this system, e.g., 4-cyclohexyl-1-(4-nitrophenyl)carbonyl thiosemicarbazide

Table 4 Experimental and computed (raw and scaled) IR frequencies for the most stable tautomer 01 of compounds **1–9**

Comp.	IR frequencies (cm^{-1})														
	N-NH[7]			**N-NH**[9]			**N-NH**[10]			**C = S**			**C = O**		
	Exp.	Comp.		Exp.	Comp.		Exp.	Comp.		Exp.	Comp.		Exp	Comp.	
		Raw	Scaled		Raw	Scaled		Raw	Scaled		Raw	Scaled		Raw	Scaled
1	3296	3577	3462	3238	3504	3392	3207	3458	3347	1306	1356	1313	1655	1724	1669
2	3328	3573	3459	3291	3497	3385	3230	3469	3357	1324	1349	1306	1664	1731	1676
3	3271	3547	3433	3242	3508	3395	3195	3466	3354	1299	1357	1313	1655	1731	1675
4	3271	3577	3462	3244	3505	3392	3189	3444	3334	1296	1358	1314	1653	1702	1648
5	3316	3575	3460	3237	3505	3393	3204	3466	3354	1297	1349	1306	1657	1706	1652
6	3314	3547	3433	3150	3513	3400	3088	3462	3351	1302	1357	1314	1701	1706	1651
7	3224	3577	3462	3097	3511	3398	2937	3452	3341	1298	1365	1321	1667	1703	1649
8	3238	3574	3459	3265	3511	3398	3101	3471	3359	1307	1349	1306	1663	1707	1652
9	3310	3545	3431	3117	3519	3406	2954	3468	3357	1302	1359	1316	1677	1707	1652

[21], 4-(2,4-dichlorophenyl)-1-(pyridin-2-yl)carbonyl thiosemicarbazide **(3)**, 4-(4-methylthiophenyl)-1-(pyridin-3-yl) carbonyl thiosemicarbazide **(4)**, 4-(2,4-dichlorophenyl)-1-(pyridin-3-yl)carbonyl thiosemicarbazide **(6)**, 4-(2-fluorophenyl)-1-(pyridin-4-yl)carbonyl thiosemicarbazide, and 4-(2-chlorophenyl)-1-(pyridin-4-yl)carbonyl-thiosemicarbazide [76]. All these compounds exist in the crystalline state in the tautomeric N1-amino/N3-amino/N4-amino/S2-thione/O5-keto form the same as compound **9**.

A search of the Cambridge Structural Database (CSD; version 5.43; November 2021, [77]) for the presence of the carbonyl thiosemicarbazide system in organic molecules (restrictions applied: $R \leq 0.1$, only non-disordered, no errors, not polymeric, no ions) revealed 102 crystal structures with this system. In all these structures, the carbonyl thiosemicarbazide system is in the N-amino/S-thione/O-keto 01 tautomeric form (Fig. 1). It should be noted that there are three crystal structures in the CSD with the carbonyl thiosemicarbazide system in the ionic structure: imidazolium N-(naphthalen-1-ylcarbamothioyl)-3,5-dinitrobenzenecarbohydrazonate, hexamethylenetetraminium N-(naphthalen-1-ylcarbamothioyl)-3,5-dinitrobenzenecarbohydra zonate, and triethylammonium N-(naphthalen-1-ylcarbamothioyl)-3,5-dinitrobenzene carbohydrazonate with the Refcodes MATLIE, MATLOK, and MATLUQ, respectively, and only in these structures the carbonyl thiosemicarbazide system appears in a different tautomeric form, namely, N1-amino/S3-thione/N4-amino/N5-imino/O7-hydroxy, 02 tautomeric form (Fig. 1).

In summarizing the results of X-ray studies of the crystal structures of compounds containing the carbonyl thiosemicarbazide system, it can be stated that the organic compounds containing this system occur in the 01 tautomeric form in the crystalline state. Only in the case of ionization of the oxygen atom of the carbonyl thiosemicarbazide system, the tautomeric equilibrium shifts towards the tautomeric form 02.

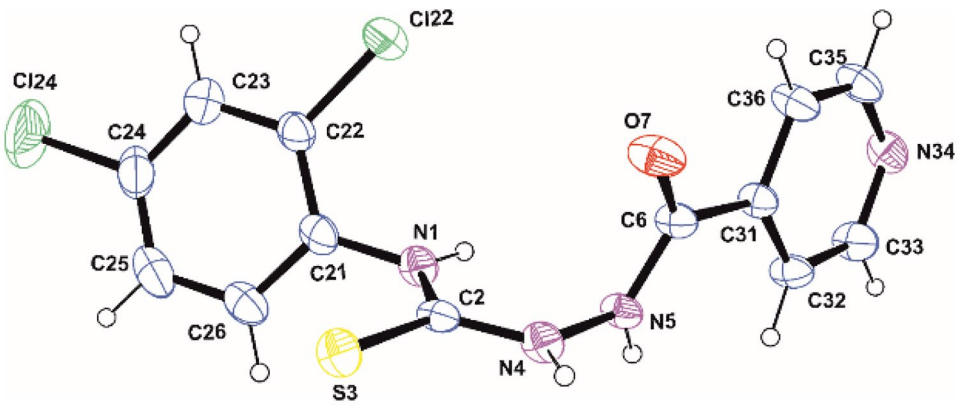

Fig. 5 The molecular structure of **9** with atom labeling and displacement ellipsoids (30% probability level)

Conclusion

The experimental and theoretical studies of 1- (2-, 3- and 4-pyridinecarbonyl)-4-substituted thiosemicarbazide derivatives have shown that the most stable tautomeric form contains a carbonyl and thione group. The obtained data broaden the knowledge of the tautomerism of thiosemicarbazide derivatives and can be used for the rational design of new therapeutic compounds.

Supplementary Information The online version contains supplementary material available at https://doi.org/10.1007/s11224-023-02152-w.

Acknowledgements These studies were carried out as part of the Statutory Activity of the Medical University of Lublin, DS 16.

Author contribution P.K.: manuscript writing, optimization of molecular geometry, calculation of stabilization energy and spectral shifts, analysis of spectroscopic spectra, and corresponding author; A.K.: optimization of molecular geometry; calculation of stabilization energies, spectral shifts, HOMO–LUMO orbitals, electrostatic potential, and non-covalent interactions; and analysis of spectra spectroscopy; Z.K.: calculation of HOMO–LUMO orbitals and Boltzmann distribution, crystal formation, X-ray structure analysis and solution of the crystal structure, and writing the manuscript; W.W.: calculation of HOMO–LUMO orbitals and Boltzmann distribution, crystal formation, X-ray structure analysis and solution of the crystal structure, and writing the manuscript; M.P.: writing the manuscript and substantive supervision.

Funding Calculations were partially performed under a computational grant by the Interdisciplinary Center for Mathematical and Computational Modeling (ICM), Warsaw, Poland, grant number G85-948.

Data availability All data generated or analyzed during this study are included in this published article (and its supplementary information files).

Declarations

Ethics approval Not applicable.

Competing interests The authors declare no competing interests.

References

1. Silverman RB, Holladay MW (2014) Chapter 1 - Introduction. In: Silverman RB, Holladay MW (eds) The organic chemistry of drug design and drug action, 3rd edn. Academic Press, Boston, pp 1–17
2. McKinney JD, Richard A, Waller C et al (2000) The practice of structure activity relationships (SAR) in toxicology. Toxicol Sci 56:8–17. https://doi.org/10.1093/toxsci/56.1.8
3. Roy K, Das RN (2014) A review on principles, theory and practices of 2D-QSAR. Curr Drug Metab 15:346–379. https://doi.org/10.2174/1389200215666140908102230
4. Patrick GL (2017) An introduction to medicinal chemistry, Oxford University Press, 2017 (ISBN:9780198749691)
5. Singh S (2000) Chemistry, design, and structure−activity relationship of cocaine antagonists. Chem Rev 100:925–1024. https://doi.org/10.1021/cr9700538
6. Antonov L (2019) Tautomerism in azo and azomethyne dyes: when and if theory meets experiment. Molecules 24:2252. https://doi.org/10.3390/molecules24122252
7. Martin YC (2009) Let's not forget tautomers. J Comput Aided Mol Des 23:693. https://doi.org/10.1007/s10822-009-9303-2
8. Dobosz R, Mućko J, Gawinecki R (2020) Using Chou's 5-step rule to evaluate the stability of tautomers: susceptibility of 2-[(phenylimino)-methyl]-cyclohexane-1,3-diones to tautomerization based on the calculated Gibbs free energies. Energies 13:183. https://doi.org/10.3390/en13010183
9. Nawrot-Modranka J, Nawrot E, Graczyk J (2006) In vivo antitumor, in vitro antibacterial activity and alkylating properties of phosphorohydrazine derivatives of coumarin and chromone. Eur J Med Chem 41:1301–1309. https://doi.org/10.1016/j.ejmech.2006.06.004
10. Sztanke K, Fidecka S, Kędzierska E et al (2005) Antinociceptive activity of new imidazolidine carbonyl derivatives.: part 4. Synthesis and pharmacological activity of 8-aryl-3,4-dioxo-2H,8H–6,7-dihydroimidazo[2,1-c] [1,2,4]triazines. Eur J Med Chem 40:127–134. https://doi.org/10.1016/j.ejmech.2004.09.020
11. Temperini C, Cecchi A, Scozzafava A, Supuran CT (2009) Carbonic anhydrase inhibitors. Comparison of chlorthalidone and indapamide X-ray crystal structures in adducts with isozyme II: when three water molecules and the keto−enol tautomerism make the difference. J Med Chem 52:322–328. https://doi.org/10.1021/jm801386n
12. Zborowski K, Korenova A, Uher M, Proniewicz LM (2004) Quantum chemical studies on tautomeric equilibria in chlorokojic and azidokojic acids. J Mol Struct Theochem 683:15–22. https://doi.org/10.1016/j.theochem.2004.06.007
13. Matosiuk D, Fidecka S, Antkiewicz-Michaluk L et al (2001) Synthesis and pharmacological activity of new carbonyl derivatives of 1-aryl-2-iminoimidazolidine: part 1. Synthesis and pharmacological activity of chain derivatives of 1-aryl-2-iminoimidazolidine containing urea moiety. Eur J Med Chem 36:783–797. https://doi.org/10.1016/S0223-5234(01)01267-3
14. Matosiuk D, Fidecka S, Antkiewicz-Michaluk L et al (2002) Synthesis and pharmacological activity of new carbonyl derivatives of 1-aryl-2-iminoimidazolidine: part 2. Synthesis and pharmacological activity of 1,6-diaryl-5,7(1H)dioxo-2,3-dihydroimidazo[1,2-a][1,3,5]triazines. Eur J Med Chem 37:761–772. https://doi.org/10.1016/S0223-5234(02)01408-3
15. Matosiuk D, Fidecka S, Antkiewicz-Michaluk L et al (2002) Synthesis and pharmacological activity of new carbonyl derivatives of 1-aryl-2-iminoimidazolidine: part 3. Synthesis and pharmacological activity of 1-aryl-5,6(1H)dioxo-2,3-dihydroimidazo[1,2-a]imidazoles. Eur J Med Chem 37:845–853. https://doi.org/10.1016/S0223-5234(02)01407-1
16. Pitucha M, Karczmarzyk Z, Wysocki W et al (2011) Experimental and theoretical investigations on the keto–enol tautomerism of 4-substituted 3-[1-methylpyrrol-2-yl)methyl]-4,5-dihydro-1H-1,2,4-triazol-5-one derivatives. J Mol Struct 994:313–320. https://doi.org/10.1016/j.molstruc.2011.03.041
17. Senthilkumar K, Kolandaivel P (2002) Quantum chemical studies on tautomerism of barbituric acid in gas phase and in solution. J Comput Aided Mol Des 16:263–272. https://doi.org/10.1023/A:1020273219651

18. Temperini C, Cecchi A, Scozzafava A, Supuran CT (2009) Carbonic anhydrase inhibitors. Comparison of chlorthalidone, indapamide, trichloromethiazide, and furosemide X-ray crystal structures in adducts with isozyme II, when several water molecules make the difference. Bioorg Med Chem 17:1214–1221. https://doi.org/10.1016/j.bmc.2008.12.023
19. Jayaram PN, Roy G, Mugesh G (2008) Effect of thione—thiol tautomerism on the inhibition of lactoperoxidase by anti-thyroid drugs and their analogues. J Chem Sci 120:143–154. https://doi.org/10.1007/s12039-008-0017-0
20. Acharya PT, Bhavsar ZA, Jethava DJ et al (2021) A review on development of bio-active thiosemicarbazide derivatives: recent advances. J Mol Struct 1226:129268. https://doi.org/10.1016/j.molstruc.2020.129268
21. Pitucha M, Woś M, Miazga-Karska M et al (2016) Synthesis, antibacterial and antiproliferative potential of some new 1-pyridinecarbonyl-4-substituted thiosemicarbazide derivatives. Med Chem Res 25:1666–1677. https://doi.org/10.1007/s00044-016-1599-6
22. Wos M, Miazga-Karska M, Kaczor AA et al (2017) Novel thiosemicarbazide derivatives with 4-nitrophenyl group as multi-target drugs: α-glucosidase inhibitors with antibacterial and antiproliferative activity. Biomed Pharmacother 93:1269–1276. https://doi.org/10.1016/j.biopha.2017.07.049
23. Pitucha M, Korga-Plewko A, Kozyra P et al (2020) 2,4-Dichlorophenoxyacetic thiosemicarbazides as a new class of compounds against stomach cancer potentially intercalating with DNA. Biomolecules 10:296. https://doi.org/10.3390/biom10020296
24. Kozyra P, Korga-Plewko A, Karczmarzyk Z et al (2022) Potential anticancer agents against melanoma cells based on an as-synthesized thiosemicarbazide derivative. Biomolecules 12:151. https://doi.org/10.3390/biom12020151
25. Kosikowska U, Wujec M, Trotsko N et al (2021) Antibacterial activity of fluorobenzoylthiosemicarbazides and their cyclic analogues with 1,2,4-triazole scaffold. Molecules 26:170. https://doi.org/10.3390/molecules26010170
26. Abu-Melha S (2018) Pyridyl thiosemicarbazide: synthesis, crystal structure, DFT/B3LYP, molecular docking studies and its biological investigations. Chem Cent J 12:101. https://doi.org/10.1186/s13065-018-0469-3
27. Ameryckx A, Thabault L, Pochet L et al (2018) 1-(2-Hydroxybenzoyl)-thiosemicarbazides are promising antimicrobial agents targeting d-alanine-d-alanine ligase in bacterio. Eur J Med Chem 159:324–338. https://doi.org/10.1016/j.ejmech.2018.09.067
28. Ameryckx A, Pochet L, Wang G et al (2020) Pharmacomodulations of the benzoyl-thiosemicarbazide scaffold reveal antimicrobial agents targeting d-alanyl-d-alanine ligase in bacterio. Eur J Med Chem 200:112444. https://doi.org/10.1016/j.ejmech.2020.112444
29. Vakulskaya TI, Larina LI, Protsuk NI, Lopyrev VA (2009) Tautomerism of 3-nitro-1,2,4-triazole-5-one radical anions. Magn Reson Chem 47:716–719. https://doi.org/10.1002/mrc.2451
30. Davari MD, Bahrami H, Haghighi ZZ, Zahedi M (2010) Quantum chemical investigation of intramolecular thione-thiol tautomerism of 1,2,4-triazole-3-thione and its disubstituted derivatives. J Mol Model 16:841–855. https://doi.org/10.1007/s00894-009-0585-z
31. Shiroudi A, Safaei Z, Kazeminejad Z et al (2020) DFT study on tautomerism and natural bond orbital analysis of 4-substituted 1,2,4-triazole and its derivatives: solvation and substituent effects. J Mol Model 26:57. https://doi.org/10.1007/s00894-020-4316-9
32. Ostakhov SS, Ovchinnikov MYu, Masyagutova GA, Khursan SL (2019) Luminescent and DFT study of keto–enol tautomers of 5-fluorouracil and its derivatives in aqueous solutions. J Phys Chem A 123:7956–7964. https://doi.org/10.1021/acs.jpca.9b04701
33. Jana K, Ganguly B (2018) DFT study to explore the importance of ring size and effect of solvents on the keto–enol tautomerization process of α- and β-cyclodiones. ACS Omega 3:8429–8439. https://doi.org/10.1021/acsomega.8b01008
34. Umadevi V, Mano Priya A, Senthilkumar L (2015) DFT study on the tautomerism of organic linker 1H-imidazole-4,5-tetrazole (HIT). Comput Theor Chem 1068:149–159. https://doi.org/10.1016/j.comptc.2015.06.022
35. Kaczor AA, Wróbel T, Karczmarzyk Z et al (2013) Experimental and computational studies on the tautomerism of N-substituted 3-amino-5-oxo-4-phenyl-1H-pyrazolo-1-carboxamides with antibacterial activity. J Mol Struct 1051:188–196. https://doi.org/10.1016/j.molstruc.2013.08.010
36. Schnell JR, Chou JJ (2008) Structure and mechanism of the M2 proton channel of influenza A virus. Nature 451:591–595. https://doi.org/10.1038/nature06531
37. Berardi MJ, Shih WM, Harrison SC, Chou JJ (2011) Mitochondrial uncoupling protein 2 structure determined by NMR molecular fragment searching. Nature 476:109–113. https://doi.org/10.1038/nature10257
38. OuYang B, Xie S, Berardi MJ et al (2013) Unusual architecture of the p7 channel from hepatitis C virus. Nature 498:521–525. https://doi.org/10.1038/nature12283
39. Oxenoid K, Dong Y, Cao C et al (2016) Architecture of the mitochondrial calcium uniporter. Nature 533:269–273. https://doi.org/10.1038/nature17656
40. Dev J, Park D, Fu Q et al (2016) Structural basis for membrane anchoring of HIV-1 envelope spike. Science 353:172–175. https://doi.org/10.1126/science.aaf7066
41. Wang G, Wang J, Nie H et al (2013) Experimental and theoretical investigations on the tautomerism of 1-phenyl-2-thiobarbituric acid and its methylation reaction. J Mol Struct 1036:372–379. https://doi.org/10.1016/j.molstruc.2012.12.017
42. Sarac K, Orek C, Koparir P (2021) Experimental and theoretical investigations regarding the thione–thiol tautomerism in 4-benzyl-5-(thiophene-2-yl)-2,4-dihydro-3H-1,2,4-triazole-3-thione. Russ J Org Chem 57:100–107. https://doi.org/10.1134/S1070428021010140
43. Becke AD (1993) Density-functional thermochemistry. III. The role of exact exchange. J Chem Phys 98:5648–5652. https://doi.org/10.1063/1.464913
44. Lee C, Yang W, Parr RG (1988) Development of the Colle-Salvetti correlation-energy formula into a functional of the electron density. Phys Rev B 37:785–789. https://doi.org/10.1103/PhysRevB.37.785
45. Frisch MJ, Trucks GW, Schlegel HB et al (2016) Gaussian 09, Revision A.02. Gaussian, Inc., Wallingford CT. https://gaussian.com/g09citation/. Accessed 3 Jan 2023
46. Miertuš S, Scrocco E, Tomasi J (1981) Electrostatic interaction of a solute with a continuum. A direct utilizaion of AB initio molecular potentials for the prevision of solvent effects. Chem Phys 55:117–129. https://doi.org/10.1016/0301-0104(81)85090-2
47. Tomasi J, Mennucci B, Cammi R (2005) Quantum mechanical continuum solvation models. Chem Rev 105:2999–3094. https://doi.org/10.1021/cr9904009
48. Keith TA, Bader RFW (1992) Calculation of magnetic response properties using atoms in molecules. Chem Phys Lett 194:1–8. https://doi.org/10.1016/0009-2614(92)85733-Q
49. Keith TA, Bader RFW (1993) Calculation of magnetic response properties using a continuous set of gauge transformations. Chem Phys Lett 210:223–231. https://doi.org/10.1016/0009-2614(93)89127-4
50. Cheeseman JR, Trucks GW, Keith TA, Frisch MJ (1996) A comparison of models for calculating nuclear magnetic resonance shielding tensors. J Chem Phys 104:5497–5509. https://doi.org/10.1063/1.471789
51. CCCBDB Vibrational frequency scaling factors. https://cccbdb.nist.gov/vsf.asp. Accessed 3 Jan 2023
52. Thompson MA (2004) Molecular Docking Using ArgusLab, an Efficient Shape-Based Search Algorithm and the a Score Scoring Function. ACS Meeting, Philadelphia. ArgusLab. http://www.arguslab.com/arguslab.com/ArgusLab.html. Accessed 3 Jan 2023

53. Contreras-García J, Johnson ER, Keinan S et al (2011) NCIPLOT: a program for plotting noncovalent interaction regions. J Chem Theory Comput 7:625–632. https://doi.org/10.1021/ct100641a
54. Humphrey W, Dalke A, Schulten K (1996) VMD: Visual molecular dynamics. J Mol Graph 14:33–38. https://doi.org/10.1016/0263-7855(96)00018-5
55. Pitucha M, Sobotka-Polska K, Keller R et al (2016) Synthesis and structure of new 1-cyanoacetyl-4-arylsemicarbazide derivatives with potential anticancer activity. J Mol Struct 1104:24–32. https://doi.org/10.1016/j.molstruc.2015.09.025
56. Agilent (2015) CrysAlisPro, Version 1.171.37.35h. Agilent Technologies Ltd, Yarnton, Oxfordshire, England
57. Sheldrick GM (2008) A short history of SHELX. Acta Cryst A 64:112–122. https://doi.org/10.1107/S0108767307043930
58. Spek AL (2015) PLATON SQUEEZE: a tool for the calculation of the disordered solvent contribution to the calculated structure factors. Acta Cryst C 71:9–18. https://doi.org/10.1107/S2053229614024929
59. Farrugia LJ (2012) WinGX and ORTEP for Windows: an update. J Appl Cryst 45:849–854. https://doi.org/10.1107/S0021889812029111
60. Pachuta-Stec A, Kosikowska U, Mazur L et al (2014) Synthesis, characterization and evaluation of antimicrobial and antituberculosis activities of new n-(substituted-thioureido)aminobicyclo dicarboximide and 3,4-disubstituted 1,2,4-triazolino-5-thione. J Chin Chem Soc 61:369–376. https://doi.org/10.1002/jccs.201300362
61. Pitucha M, Mazur L, Kosikowska U et al (2010) Synthesis, structure, and antibacterial evaluation of new N-substituted-3-amino-5-oxo-4-phenyl-2,5-dihydro-1H-pyrazole-1-carbothioamides. Heteroat Chem 21:215–221. https://doi.org/10.1002/hc.20598
62. Cihan-Üstündağ G, Gürsoy E, Naesens L et al (2016) Synthesis and antiviral properties of novel indole-based thiosemicarbazides and 4-thiazolidinones. Bioorg Med Chem 24:240–246. https://doi.org/10.1016/j.bmc.2015.12.008
63. Dzitko K, Paneth A, Plech T et al (2014) 1,4-Disubstituted thiosemicarbazide derivatives are potent inhibitors of Toxoplasma gondii proliferation. Molecules 19:9926–9943. https://doi.org/10.3390/molecules19079926
64. Paneth A, Plech T, Kaproń B et al (2016) Design, synthesis and biological evaluation of 4-benzoyl-1-dichlorobenzoylthiosemicarbazides as potent Gram-positive antibacterial agents. J Enzyme Inhib Med Chem 31:434–440. https://doi.org/10.3109/14756366.2015.1036050
65. Abhale YK, Shinde A, Deshmukh KK et al (2017) Synthesis, antitubercular and antimicrobial potential of some new thiazole substituted thiosemicarbazide derivatives. Med Chem Res 26:2557–2567. https://doi.org/10.1007/s00044-017-1955-1
66. Miar M, Shiroudi A, Pourshamsian K et al (2021) Theoretical investigations on the HOMO–LUMO gap and global reactivity descriptor studies, natural bond orbital, and nucleus-independent chemical shifts analyses of 3-phenylbenzo[d]thiazole-2(3H)-imine and its para-substituted derivatives: Solvent and substituent effects. J Chem Res 45:147–158. https://doi.org/10.1177/1747519820932091
67. Fukui K, Yonezawa T, Shingu H (1952) A molecular orbital theory of reactivity in aromatic hydrocarbons. J Chem Phys 20:722–725. https://doi.org/10.1063/1.1700523
68. Rathi PC, Ludlow RF, Verdonk ML (2020) Practical high-quality electrostatic potential surfaces for drug discovery using a graph-convolutional deep neural network. J Med Chem 63:8778–8790. https://doi.org/10.1021/acs.jmedchem.9b01129
69. Kulabaş N, Tatar E, Bingöl Özakpınar Ö et al (2016) Synthesis and antiproliferative evaluation of novel 2-(4H–1,2,4-triazole-3-ylthio) acetamide derivatives as inducers of apoptosis in cancer cells. Eur J Med Chem 121:58–70. https://doi.org/10.1016/j.ejmech.2016.05.017
70. Küçükgüzel G, Kocatepe A, De Clercq E et al (2006) Synthesis and biological activity of 4-thiazolidinones, thiosemicarbazides derived from diflunisal hydrazide. Eur J Med Chem 41:353–359. https://doi.org/10.1016/j.ejmech.2005.11.005
71. Pitucha M, Karczmarzyk Z, Kosikowska U, Malm A (2011) Synthesis, experimental and theoretical study on the structure of some semicarbazides with potential antibacterial activity. Z Naturforsch B 66:505–511. https://doi.org/10.1515/znb-2011-0511
72. Sardari S, Feizi S, Rezayan AH et al (2017) Synthesis and biological evaluation of thiosemicarbazide derivatives endowed with high activity toward Mycobacterium bovis. Iran J Pharm Res 16:1128–1140
73. Yamaguchi MU, Barbosa da Silva AP, Ueda-Nakamura T et al (2009) Effects of a thiosemicarbazide camphene derivative on Trichophyton mentagrophytes. Molecules 14:1796–1807. https://doi.org/10.3390/molecules14051796
74. Salgın-Gökşen U, Gökhan-Kelekçi N, Göktaş Ö et al (2007) 1-Acylthiosemicarbazides, 1,2,4-triazole-5(4H)-thiones, 1,3,4-thiadiazoles and hydrazones containing 5-methyl-2-benzoxazolinones: synthesis, analgesic-anti-inflammatory and antimicrobial activities. Bioorg Med Chem 15:5738–5751. https://doi.org/10.1016/j.bmc.2007.06.006
75. Allen FH, Kennard O, Watson DG et al (1987) Tables of bond lengths determined by X-ray and neutron diffraction. Part 1. Bond lengths in organic compounds. J Chem Soc, Perkin Trans 2:S1–S19. https://doi.org/10.1039/P298700000S1
76. Pitucha M, Karczmarzyk Z, Swatko-Ossor M et al (2019) Synthesis, in vitro screening and docking studies of new thiosemicarbazide derivatives as antitubercular agents. Molecules 24:251. https://doi.org/10.3390/molecules24020251
77. Groom CR, Bruno IJ, Lightfoot MP, Ward SC (2016) The Cambridge Structural Database. Acta Cryst B 72:171–179. https://doi.org/10.1107/S2052520616003954